THE EFFECT OF THERMAL FIELDS ON THE DENSITY AND DISTRIBUTION OF DISLOCATION IN SEMI-TRANSPARENT SINGLE CRYSTALS PULLED BY THE CZOCHRALSKI TECHNIQUE

By E. Zalewski

Research and Development Centre of Television Engineering, Warsaw*

and J. Żmija

Institute of Technical Physics, Military Technical Academy, Warsaw**

(Received December 18, 1979; revised version received April 26, 1980; final version received June 12, 1980)

High thermal gradients occurring in the Czochralski technique of crystal growth are directly responsible for the existence of specific thermoelastic stress distributions in a solid phase. Thus they are responsible for the distribution of elastic energy density and dislocations. In this work, calculations of the distribution and density of thermoelastic stress energy and dislocations are presented. The calculations for lithium niobate and yttrium-aluminum garnet single crystals are made. The theoretical data are in good agreement with the experimental results.

PACS numbers: 62.20.Fe, 61.50.Cj, 61.70.Ga

1. Introduction

Temperature distribution in semi-transparent single crystals pulled by the Czochralski technique may be approximated by the hyperbolic function (sinh z or cosh z) in an axial direction and by the Bessel first kind function in a radial direction [1]. A similar behaviour reveals components of the thermoelastic stress [2, 3].

Temperature gradients promote generation of dislocations in the crystals. Correlations for the two values had been attempted before [4, 5]. However, the explanation of the dislocation generation process was based on the geometric factors. The calculations of dislocation density issued from the difference of line dimensions of a single crystal stratum due to temperature differences.

* Address: Centrum Naukowo-Produkcyjne Techniki Telewizyjnej, Długa 44/50, 00-241 Warszawa, Poland.

** Address: Wojskowa Akademia Techniczna, Lazurowa 225, 01-489 Warszawa, Poland.

Thermal gradients and thermoelastic stresses promote the generation of dislocations in crystals only indirectly, we presume. The direct cause involves the density of thermoelastic stress energy and the crystal tendency to minimize this energy.

Because of this, we calculate the density and distribution of dislocations in a single crystal from an energy point of view. We assume that the line defect originates at the points where the density of thermoelastic stress energy is over the value of the threshold energy for dislocation generation.

2. *Distribution of density of thermoelastic stress energy*

We calculate the energy following the usual expression

$$W = \sigma_i \varepsilon_i = c_{ij} \varepsilon_i \varepsilon_j = s_{ij} \sigma_i \sigma_j, \tag{1}$$

where W — density of thermoelastic stress energy, σ_i — component of stress, ε_i — component of strain, c_{ij}, s_{ij} — coefficients of elasticity. In the case of the cylindrical coordinate system expression (1) will change as follows:

$$W = \tfrac{1}{2} s'_{11}(\sigma_{rr}^2 + \sigma_{\varphi\varphi}^2) + \tfrac{1}{2} s'_{33}\sigma_{zz}^2 + \tfrac{1}{2} s'_{55}\sigma_{rz}^2 + s'_{12}\sigma_{rr}\sigma_{\varphi\varphi} + \tfrac{1}{2} s'_{13}\sigma_{zz}(\sigma_{rr} + \sigma_{\varphi\varphi}), \tag{2}$$

where s'_{ij} are the coefficients of rigidity converted to the cylindrical system. The transformation formulas communicated by Lechnicki [6] were used. Table I shows the numerical values of s'_{ij} foc $LiNbO_3$ and $Y_3Al_5O_{12}$.

TABLE I

Numerical values for $LiNbO_3$ and $Y_3Al_5O_{12}$ rigidity coefficients

Coefficient	Value $[10^{-12}$ cm^2/dyn]	
	$LiNbO_3$	$Y_3Al_5O_{12}$
s'_{11}	0.5831	0.3519
s'_{33}	0.5026	0.3591
s'_{33}	1.710	0.8688
s'_{12}	−0.1150	−0.0825
s'_{13}	−0.1452	−0.0897

Numerical calculations of the distribution of thermoelastic stress energy were made by an electronic digital computer. Mathematical expressions for stress presented previously [2] were used. The following values of technological parameters were assumed, that is a crystal having a diameter of 20 mm, a length of 50 mm, an environmental temperature of 1070 K for $LiNbO_3$ and 1270 K for YAG and melting points respectively of 1530 and 2240 K. The results are listed in Table II.

The distribution of the density of thermoelastic stress energy in the crystals may be characterized as follows:

TABLE II

Distribution of the density of thermoelastic stress energy in $LiNbO_3$ and $Y_3Al_5O_{12}$ single crystals [in erg/cm^3]

Axial direction[b] z/z_0	Radial direction[a] r/R										
	0	0.1	0.2	0.3	0.4	0.5	0.6	0.7	0.8	0.9	1.0
					lithium niobate						
0.4	6.923	6.601	1.001	2.006	1.636	1.474	14.28	21.92	11.38	11.29	16.00
0.5	6.663	6.904	2.472	4.259	3.693	2.689	14.96	23.09	13.91	15.08	18.58
0.6	8.504	9.427	6.415	9.151	8.340	6.300	17.91	26.62	19.07	21.72	22.98
0.7	13.68	15.44	14.13	18.10	17.11	13.90	24.77	34.28	28.85	33.30	30.53
0.8	20.94	23.35	24.31	30.34	30.23	26.79	37.83	49.44	47.93	55.40	44.92
0.9	20.16	22.11	22.79	30.71	33.81	34.08	51.31	76.63	97.27	126.3	92.04
					yttrium-aluminum garnet						
0.4	3485	3485	1464	1.428	1604	4954	6572	5233	3908	5472	6538
0.5	3743	3700	1580	43.87	1553	4922	6618	5400	4184	5802	6872
0.6	4069	3975	1737	104.5	1512	4904	6696	5624	4539	6219	7285
0.7	4466	4317	1947	178.0	1480	4898	6806	5923	5006	6764	7824
0.8	4809	4641	2174	120.5	1416	4818	6867	6272	5651	7561	8607
0.9	4381	4379	2116	188.0	1016	3966	6003	6140	6662	9352	10410

[a] here: r — radial coordinate, R — crystal radius,
[b] here: z — axial coordinate, $z = z_0$ at the interface.

a) It increases in the radial direction from the center to the periphery of a crystal. This is especially seen for lithium niobate in the region close to the interface. The minimum of energy density appears in yttrium-aluminum garnet due to the existence of a "neutral zone". Such "zones" occur for high differences in temperature. They were detected in leucosapphire single crystals grown by the flame fusion technique [7, 8]. For the Czochralski technique where thermal conditions of growth are much moderate, such a phenomenon is observed rarely. This minimum does not occur in $LiNbO_3$;

b) In the region of the crystal apart from the interface energy density distribution becomes more homogeneous and absolute values of the density decrease.

3. Density and distribution of dislocations

One may assume that dislocation appears at the point where stress energy density, W, overcomes the threshold energy of the defect formation, E_d. This is a result of the crystal tendency to minimize its intrinsic energy. As dislocation is formed the residual stress energy appears which can reach values of $0 \leqslant E_r \leqslant E_d$. It may be assumed that:

$$E_r \approx \tfrac{1}{2} E_d. \tag{3}$$

To form a dislocation average energy is needed that

$$E_g = \tfrac{3}{2} E_d. \tag{4}$$

So that the density of dislocations, N, is proportional to the density of stress energy:

$$N \approx 2W/3E_d \quad (\mathrm{cm}^{-3}). \tag{5}$$

The latter expression is used to calculate the dislocation density in the crystals.

E_d is the total energy of the dislocation. This involves the energy of the core as well as that of the stress field of the dislocation line. Both components may be evaluated from the known formulas. These give $\approx 10^{-2}$ erg for E_d for $LiNbO_3$ and $\approx 2 \times 10^{-2}$ erg for YAG.

4. Experimental procedures

To verify theoretical considerations the density and distribution of dislocations in lithium niobate and yttrium-aluminum garnet single crystals were measured. The crystals were pulled by the Czochralski technique in a conventional way. The only difference involved the resistance afterheater used. The rate of pulling was 6 mm/h for $LiNbO_3$ and 3 mm/h for YAG and seed rotation 40 for both. The temperature profiles in the afterheaters are shown in Fig. 1.

Dislocations were examined by the etch pit technique. We used crystal plates with plane surfaces perpendicular to the growth axis. Etch pit observation was done with an optical microscope with enlargements of 100–150 × . Observation area varied from 0.25 to 0.3 mm^2.

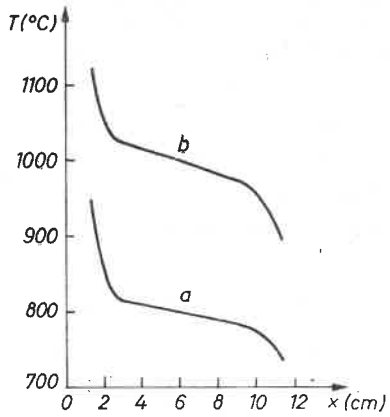

Fig. 1. Temperature distributions in afterheaters for lithium niobate *a* and yttrium-aluminum garnet *b*. In both cases measurements were held with melted charges

5. *Discussion*

The results of theoretical calculations and experimental data are presented in Table III and Fig. 2.

It should be noticed that energy density reaches its highest value at the interface. Each point of a crystal is subjected to the influence of axial stress components σ_{zz} and σ_{rz} for a certain time in which it becomes apart from the boundary region. Thus, the axial distribution of dislocations is not a factor which differentiates various volume elements of the crystal. The factor is the radial distribution of energy and dislocation densities.

TABLE III

Radial distributions of dislocation densities in lithium niobate and yttrium-aluminum garnet single crystals

r/R	Dislocation density			
	Calculated [cm^{-3}]		Measured [cm^{-2}]	
	$LiNbO_3$	$Y_3Al_5O_{12}$	$LiNbO_3$	$Y_3Al_5O_{12}$
0	1140	128×10^3	1.5×10^3	
0.1	1260	128×10^3		
0.2	1290	62×10^3		
0.25			2.0×10^3	1.4×10^4
0.3	1740	4×10^3		
0.4	1920	30×10^3		
0.5	1940	116×10^3	2.7×10^3	1.4×10^5
0.6	2910	176×10^3		
0.7	4350	180×10^3		
0.75			5.8×10^3	2.8×10^5
0.8	5520	195×10^3		
0.9	7170	274×10^3	1.3×10^4	3.1×10^5
1.0	5300	305×10^3		

As can be seen from Fig. 2, the theoretical and experimental curves correspond qualitatively to each other. The values for the average densities are of the same order of magnitude. The experimental curves lie below the theoretical curves. This results from using different units to measure the dislocation density. Calculated density is expressed by the length of dislocation lines in cm^{-3} but the measured one is then by number of etch pits in cm^{-2}. However, it is known that the density of dislocations measured in cm^{-3} is proportional to the same one as measured in cm^{-2}. This was estimated by Schoeck [9]

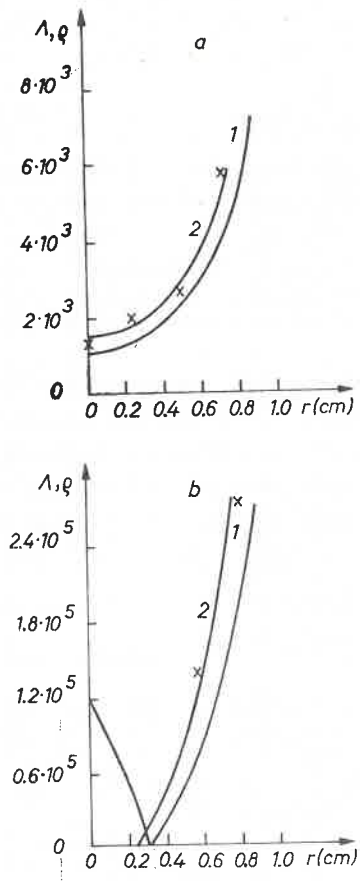

Fig. 2. Distribution of thermal dislocations in lithium niobate and yttrium-aluminum garnet single crystals. On both figures, a) for $LiNbO_3$ and b) for YAG, curve *1* indicates the theoretical calculated distribution while curve *2* indicates the distribution obtained in the experimental way by the etch pit technique

for 16 cases of regular crystal surfaces assuming an isotropic space distribution of dislocations or their isotropic distribution in one or more slide planes. When the dislocation line length in cm^{-3} is designated as Λ, and the dislocation density in cm^{-2} by ϱ, then Schoeck could assume the relation:

$$\Lambda \sim 2\varrho. \tag{6}$$

For general cases we have:

$$\Lambda \approx k\varrho. \tag{7}$$

In the cases referenced to by Schoeck, the coefficient k has values from 1.66 to 2.36. For our crystals the theoretical and experimental curves are covered when one assumes that

$$k \approx 1.2 \tag{8}$$

for lithium niobate and

$$k \approx 1.4 \tag{9}$$

for yttrium-aluminum garnet.

Thus the increase of value towards the periphery is characteristic feature of thermally generated dislocation distribution in single crystals pulled by the Czochralski technique. These results were confirmed by numerous works which saw that stress is one of the most important factors which must be eliminated to obtain good quality crystals [10–12]. Now techniques can grow free of dislocations crystal (Si), or a few dislocation pits of cm^{-2} (GGG). This is principally due to the minimization of thermal differences in the solid state.

6. Conclusion

The theory presented here facilitates the calculations of density and distribution of dislocations in semi-transparent oxide single crystals pulled by the Czochralski technique. The average value of calculated dislocation density agrees with the experimental one within 30% accuracy which should be regarded as the satisfying convergence. The quality runs of both curves are the same.

REFERENCES

[1] E. Zalewski, J. Żmija, *Acta Phys. Pol.* **A51**, 807, 819 (1977).
[2] E. Zalewski, J. Żmija, *Acta Phys. Pol.* **A53**, 503 (1978).
[3] Z. Patryas, E. Zalewski, J. Żmija, *Acta Phys. Pol.* **A53**, 773 (1978).
[4] E. Billig, *Proc. R. Soc.* (*London*) **A235**, 37 (1956).
[5] S. V. Civinskii, *Fiz. Met. Metalloved.* **25**, 1013 (1968).
[6] S. G. Lekhnitskii, *Teorya Uprugosti Anizotropnogo Tela*, Gosudarstvennoye Izdatelstvo Tekhniko-Teoreticheskoy Literatury, Moskva-Leningrad 1950.
[7] N. Yu. Ikornikova, G. Ye. Tomilovskii, *Trudy Instituta Kristallografii* **8**, 193 (1953).
[8] N. Yu. Ikornikova, *Trudy Instituta Kristallografii* **8**, 193 (1953).
[9] G. Schoeck, *J. Appl. Phys.* **33**, 1745 (1962).
[10] B. Cockayne, D. S. Robertson, W. Bardsley, *Brit. J. Appl. Phys.* **15**, 1165 (1964).
[11] R. B. Maciolek, E. Bernal, *Mater. Res. Bull.* **10**, 1355 (1975).
[12] J. C. Brice, *J. Cryst. Growth* **7**, 9 (1970).